SUPPORTING INFORMATION

Naphthalene-stilbenes as effective visible-light sensitizers to study the effect of diluent and nanofillers on in situ photopolymerization and 3D-VAT printing process

Wiktoria Tomal[1], Karolina Gałuszka[1], Petr Lepcio[2], Maciej Pilch[1], Anna Chachaj-Brekiesz[3], Martina Korčušková[2], Joanna Ortyl *[1,4]

[1] Cracow University of Technology, Faculty of Chemical Engineering and Technology, Warszawska 24, 31–155 Cracow, Poland
[2] Central European Institute of Technology, Brno University of Technology, Purkynova 656/123, Brno 612 00, Czech Republic
[3] Jagiellonian University, Faculty of Chemistry, Gronostajowa 2, 30-387 Cracow, Poland
[4] Photo HiTech Ltd., Bobrzyńskiego 14, 30–348 Cracow, Poland

*****Correspondence: joanna.ortyl@pk.edu.pl

CONTENTS

Materials and characterization of synthesized compounds

The 1-amino-6-bromo-4-methylnaphthalene-2-carbonitrile was synthesized following the literature procedure.[1] Unless otherwise noted, all organic compounds, inorganic salts and solvents were analytically pure and used as received. DMF was dried over freshly activated 4Å molecular sieves. The structure and purity of obtained products were confirmed by nuclear magnetic resonance and elemental analysis. ^{1}H NMR spectra were recorded in DMSO-D_6 on Advance III 400 MHz (Bruker) spectrometer. Chemical shifts were reported in parts per million (δ) and referenced to residual protonated solvent peak (δ=2.50 ppm for DMSO-D_6). Elemental analyses were performed with Vario EI III apparatus (Elementar).

Synthetic procedures

All target compounds (NS, NS-ME, NS-F, NS-Cl, NS-CN, NS-S-Me, NS-O-Me, NS-O-$(Me)_3$) were synthesized *via* Heck coupling of 1-amino-6-bromo-4-methylnaphthalene-2-carbonitrile with an appropriate styrene derivative. The applied synthetic protocol was already described in the literature for Heck coupling of 2-amino-4-(4-bromophenyl)-6-phenyl-benzene-1,3-dicarbonitrile.[2]

General procedure for synthesis of 1-amino-4-methyl-6-styrylnaphthalene-2-carbonitrile derivatives

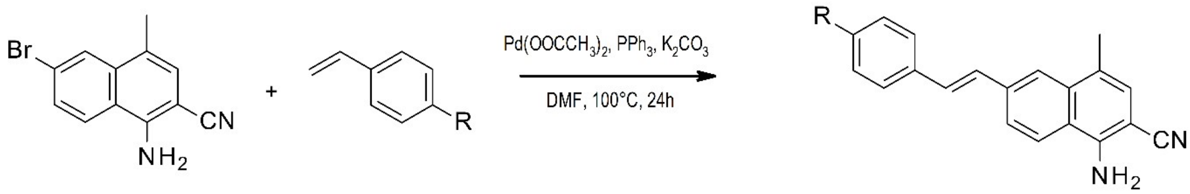

1-amino-6-bromo-4-methylnaphthalene-2-carbonitrile (150 mg, 0.57 mmol), $Pd(OOCCH_3)_2$ (10 mg, 0.045 mmol), triphenylphosphine (12 mg, 0.045 mmol), K_2CO_3 (210 mg, 1.52 mmol), appropriate styrene derivative (1.73 mmol) and anhydrous DMF (3 mL) were placed under nitrogen in the pressure vial and heated for 24 h at a temperature of 100 °C. The resulting mixture was treated with water (10 mL) and extracted with $CHCl_3$ (3 × 10 mL). Organic extracts were combined, dried over anhydrous $MgSO_4$ and concentrated under vacuum. Products were purified by column chromatography (silica gel/$CHCl_3$) followed by crystallization from $CHCl_3$/hexanes mixture.

Analytical data of the compounds used in this study

Physicochemical data of the azulene derivatives used in this study

<table>
<tr><td colspan="2">1-amino-4-methyl-6-[(E)-styryl]naphthalene-2-carbonitrile, NS</td></tr>
<tr><td>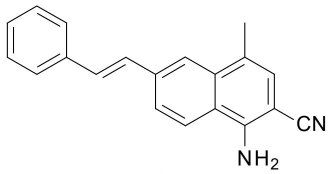
NS</td><td>Synthesized from styrene (180 mg) in 71% yield.

^{1}H NMR (400 MHz, DMSO) δ 8.34 (d, J = 8.9 Hz, 1H), 7.97 (d, J = 1.4 Hz, 1H), 7.90 (dd, J = 8.9, 1.5 Hz, 1H), 7.70 – 7.66 (m, 2H), 7.52 (d, J = 16.5 Hz, 1H), 7.47 (d, J = 16.5 Hz, 1H), 7.44 – 7.39 (m, 2H), 7.33 – 7.29 (m, 1H), 7.17 (d, J = 0.7 Hz, 1H), 6.65 (s, 2H), 2.48 (d, J = 0.7 Hz, 3H).

Anal. Calc. for $C_{20}H_{16}N_2$: C 84.48% H 5.67% N 9.85% Found: C 84.25% H 5.64% N 9.61%</td></tr>
<tr><td colspan="2">1-amino-4-methyl-6-[(E)-2-(4-methylphenyl)vinyl]naphthalene-2-carbonitrile, NS-Me</td></tr>
<tr><td>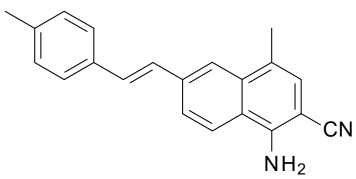
NS-Me</td><td>Synthesized from 4-metylstyrene (202 mg) in 37% yield.

1H NMR (400 MHz, DMSO) δ 8.33 (d, J = 8.9 Hz, 1H), 7.94 (d, J = 1.5 Hz, 1H), 7.88 (dd, J = 8.9, 1.5 Hz, 1H), 7.60 – 7.54 (m, 2H), 7.47 (d, J = 16.5 Hz, 1H), 7.41 (d, J = 16.5 Hz, 1H), 7.25 – 7.19 (m, 2H), 7.16 (d, J = 0.7 Hz, 1H), 6.64 (s, 2H), 2.47 (d, J = 0.7 Hz, 3H), 2.32 (s, 3H).

Anal. Calc. for C21H18N2: C 84.53% H 6.08% N 9.39% Found: C 84.67% H 5.91% N 9.56%</td></tr>
<tr><td colspan="2">1-amino-6-[(E)-2-(4-fluorophenyl)vinyl]-4-methylnaphthalene-2-carbonitrile, NS-F</td></tr>
<tr><td>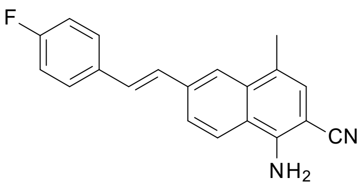
NS-F</td><td>Synthesized from 4-fluorostyrene (220 mg) in 37% yield.

^{1}H NMR (400 MHz, DMSO) δ 8.34 (d, J = 8.9 Hz, 1H), 7.95 (d, J = 1.5 Hz, 1H), 7.88 (dd, J = 8.9, 1.6 Hz, 1H), 7.76 – 7.70 (m, 2H), 7.52 (d, J = 16.5 Hz, 1H), 7.43 (d, J = 16.5 Hz, 1H), 7.28 – 7.22 (m, 2H), 7.17 (d, J = 0.8 Hz, 1H), 6.65 (s, 2H), 2.47 (d, J = 0.8 Hz, 3H).

Anal. Calc. for $C_{20}H_{15}N_2F$: C 79.45% H 5.00% N 9.27% Found: C 79.88% H 5.11% N 8.96%</td></tr>
<tr><td colspan="2">1-amino-6-[(E)-2-(4-chlorophenyl)vinyl]-4-methylnaphthalene-2-carbonitrile, NS-Cl</td></tr>
<tr><td>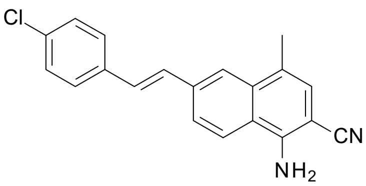
NS-Cl</td><td>Synthesized from 4-chlorostyrene (238 mg) in 23% yield.

^{1}H NMR (400 MHz, DMSO) δ 8.34 (d, J = 8.9 Hz, 1H), 7.97 (d, J = 1.6 Hz, 1H), 7.89 (dd, J = 8.9, 1.6 Hz, 1H), 7.73 – 7.67 (m, 2H), 7.51 (s, 2H), 7.49 – 7.45 (m, 2H), 7.17 (d, J = 0.8 Hz, 1H), 6.65 (s, 2H), 2.48 (d, J = 0.8 Hz, 3H).

Anal. Calc. for $C_{20}H_{15}N_2Cl$: C 74.98% H 4.66% N 8.43% Found: C 75.03% H 4.70% N 8.48%</td></tr>
<tr><td colspan="2">1-amino-6-[(E)-2-(4-cyanophenyl)vinyl]-4-methylnaphthalene-2-carbonitrile, NS-CN</td></tr>
<tr><td>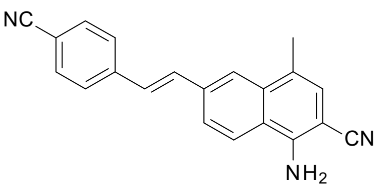
NS-CN</td><td>Synthesized from 4-cyanostyrene (220 mg) in 68% yield.

1H NMR (400 MHz, DMSO) δ 8.37 (d, J = 8.9 Hz, 1H), 8.02 (d, J = 1.4 Hz, 1H), 7.92 (dd, J = 8.9, 1.4 Hz, 1H), 7.86 (s, 4H), 7.69 (d, J = 16.5 Hz, 1H), 7.59 (d, J = 16.5 Hz, 1H), 7.18 (d, J = 0.8 Hz, 1H), 6.68 (s, 2H), 2.48 (d, J = 0.8 Hz, 3H).

Anal. Calc. for C21H15N3: C 81.53% H 4.89% N 13.58% Found: C 81.60% H 4.74% N 13.47%</td></tr>
</table>

<table>
<tr><td colspan="2">1-amino-4-methyl-6-[(E)-2-(4-methylsulfanylphenyl)vinyl]naphthalene-2-carbonitrile, NS-S-Me</td></tr>
<tr><td>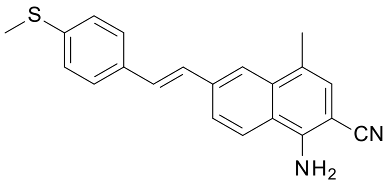
NS-S-Me</td><td>Synthesized from 4-methylsulfanylstyrene (258 mg) in 82% yield.

^{1}H NMR (400 MHz, DMSO) δ 8.33 (d, J = 8.9 Hz, 1H), 7.95 (d, J = 1.5 Hz, 1H), 7.88 (dd, J = 8.9, 1.5 Hz, 1H), 7.65 – 7.59 (m, 2H), 7.48 (d, J = 16.5 Hz, 1H), 7.43 (d, J = 16.5 Hz, 1H), 7.31 – 7.27 (m, 2H), 7.16 (d, J = 0.9 Hz, 1H), 6.64 (s, 2H), 2.51 (s, 3H), 2.47 (d, J = 0.9 Hz, 3H).

Anal. Calc. for $C_{21}H_{18}N_2S$: C 74.73% H 5.27% N 8.28% Found: C 74.80% H 5.31% N 8.33%</td></tr>
<tr><td colspan="2">1-amino-6-[(E)-2-(4-methoxyphenyl)vinyl]-4-methylnaphthalene-2-carbonitrile, NS-O-Me</td></tr>
<tr><td>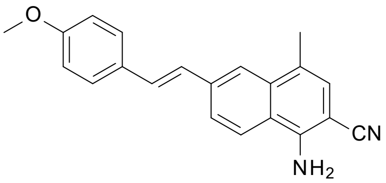
NS-O-Me</td><td>Synthesized from 4-methoxystyrene (231 mg) in 60% yield.

^{1}H NMR (400 MHz, DMSO) δ 8.32 (d, J = 8.9 Hz, 1H), 7.91 (d, J = 1.5 Hz, 1H), 7.86 (dd, J = 8.9, 1.6 Hz, 1H), 7.65 – 7.58 (m, 2H), 7.46 (d, J = 16.5 Hz, 1H), 7.32 (d, J = 16.4 Hz, 1H), 7.15 (d, J = 0.9 Hz, 1H), 7.02 – 6.95 (m, 2H), 6.63 (s, 2H), 3.79 (s, 3H), 2.47 (d, J = 0.9 Hz, 3H).

Anal. Calc. for $C_{21}H_{18}N_2O$: C 78.20% H 5.56% N 8.62% Found: C 78.26% H 5.59% N 8.66%</td></tr>
<tr><td colspan="2">1-amino-6-[(E)-2-(4-tert-butoxyphenyl)vinyl]-4-methylnaphthalene-2-carbonitrile, NS-O-(Me)$_3$</td></tr>
<tr><td>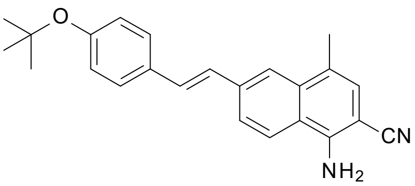
NS-O-(Me)$_3$</td><td>Synthesized from 4-tert-butoxystyrene (301 mg) in 27% yield.

^{1}H NMR (400 MHz, DMSO) δ 8.33 (d, J = 8.9 Hz, 1H), 7.93 (d, J = 1.5 Hz, 1H), 7.87 (dd, J = 8.9, 1.6 Hz, 1H), 7.62 – 7.55 (m, 2H), 7.46 (d, J = 16.4 Hz, 1H), 7.35 (d, J = 16.4 Hz, 1H), 7.16 (d, J = 0.9 Hz, 1H), 7.03 – 6.97 (m, 2H), 6.64 (s, 2H), 2.47 (d, J = 0.9 Hz, 3H), 1.32 (s, 9H).

Anal. Calc. for $C_{24}H_{24}N_2O$: C 80.08% H 6.71% N 7.74% Found: C 80.04% H 6.68% N 7.70%</td></tr>
</table>

NMR spectra of the compounds used in this study

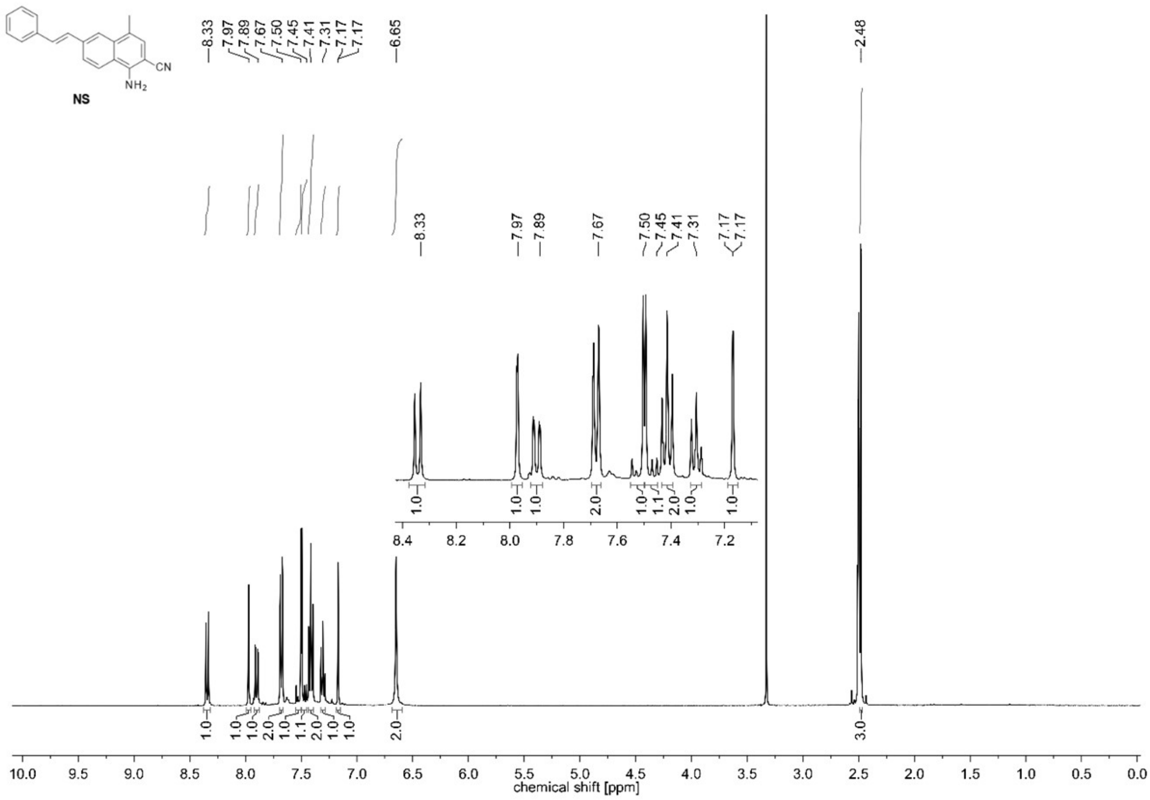

Figure S1. [1]HNMR spectrum of 1-amino-4-methyl-6-[(E)-styryl]naphthalene-2-carbonitrile, **NS**.

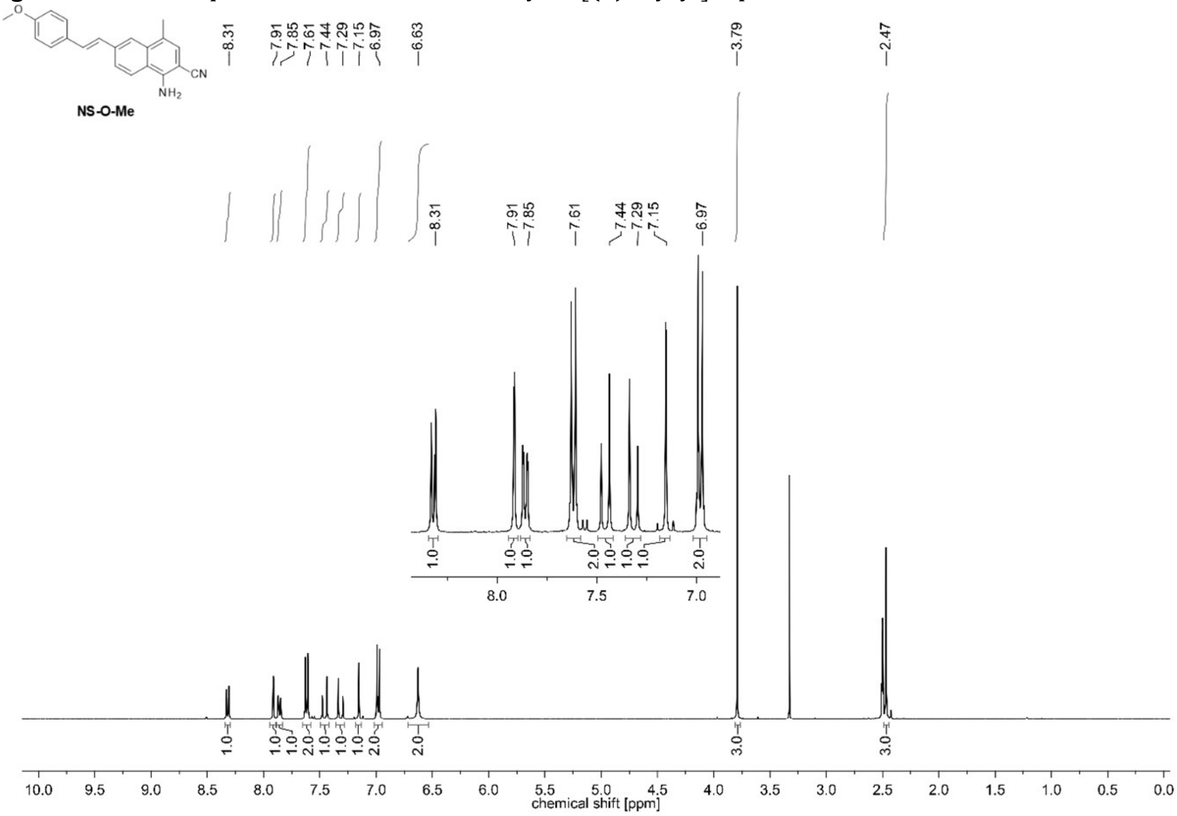

Figure S2. [1]HNMR spectrum of 1-amino-4-methyl-6-[(E)-2-(4-methylphenyl)vinyl]naphthalene-2-carbonitrile, **NS-Me**.

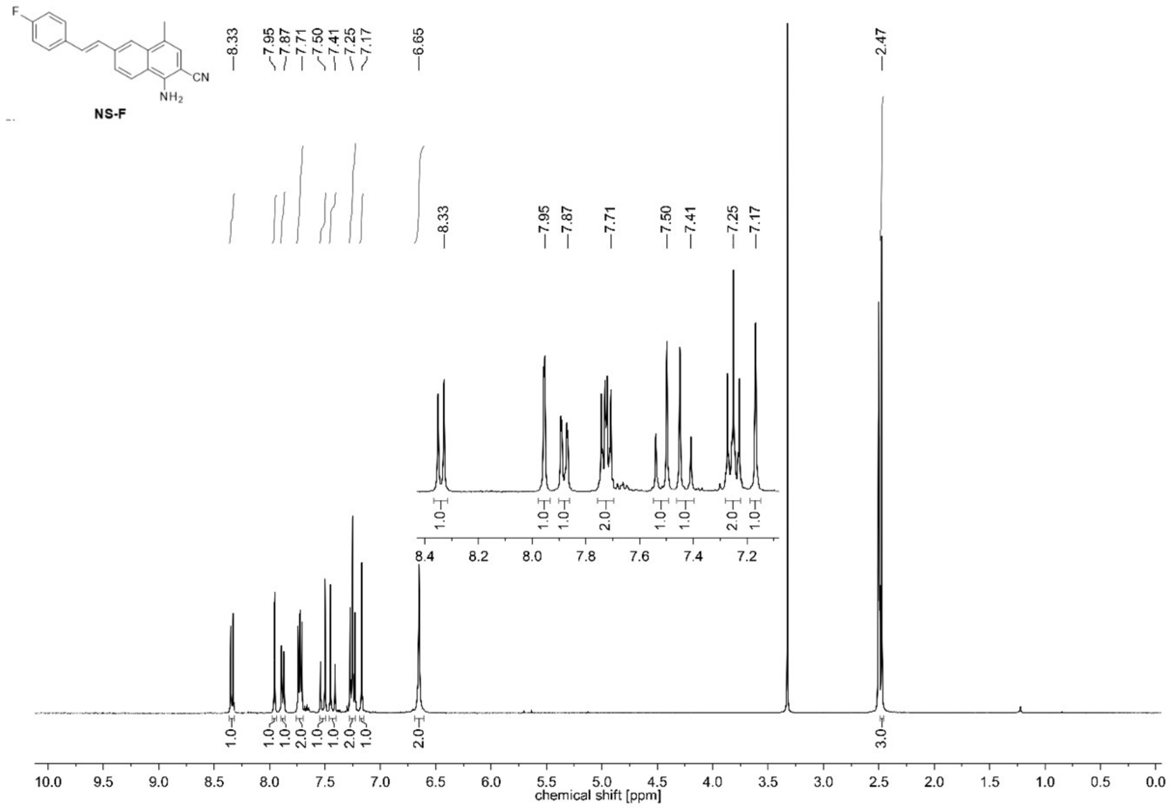

Figure S3. ^{1}HNMR spectrum of1-amino-6-[(E)-2-(4-fluorophenyl)vinyl]-4-methylnaphthalene-2-carbonitrile, **NS-F**.

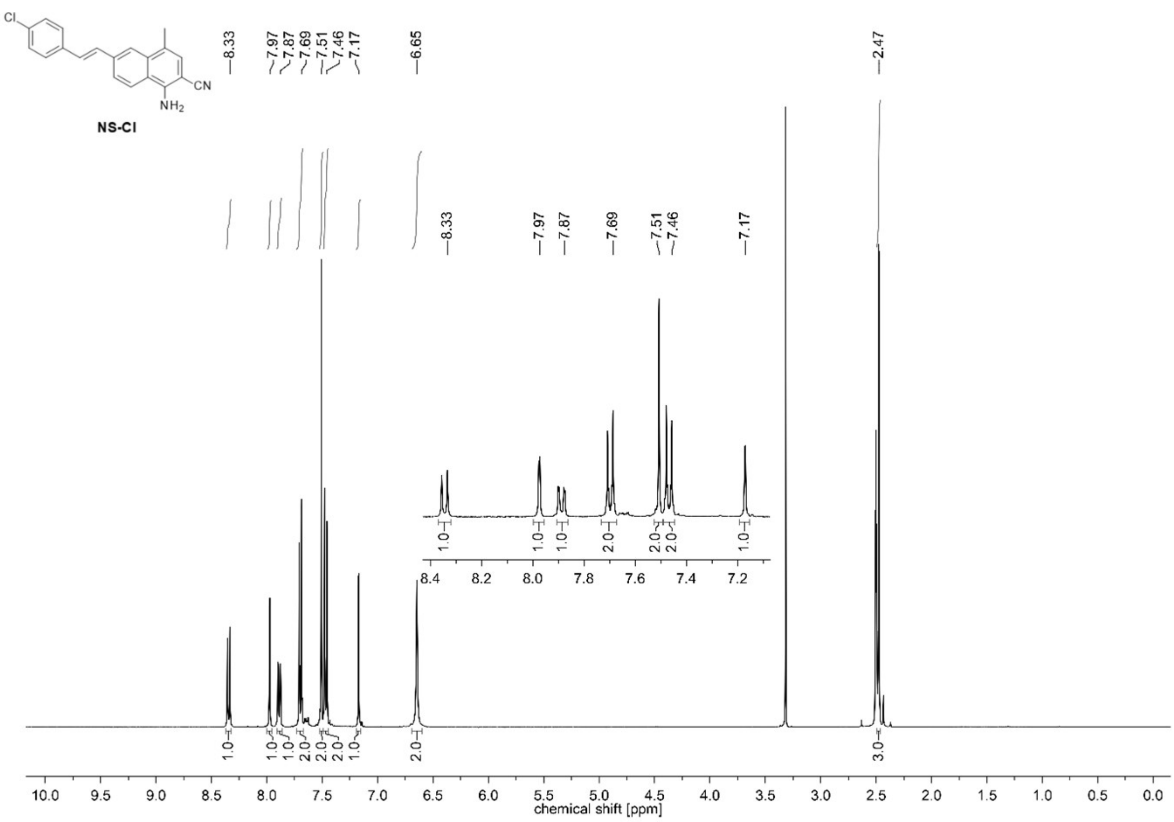

Figure S4. ^{1}HNMR spectrum of 1-amino-6-[(E)-2-(4-chlorophenyl)vinyl]-4-methylnaphthalene-2-carbonitrile, **NS-Cl**.

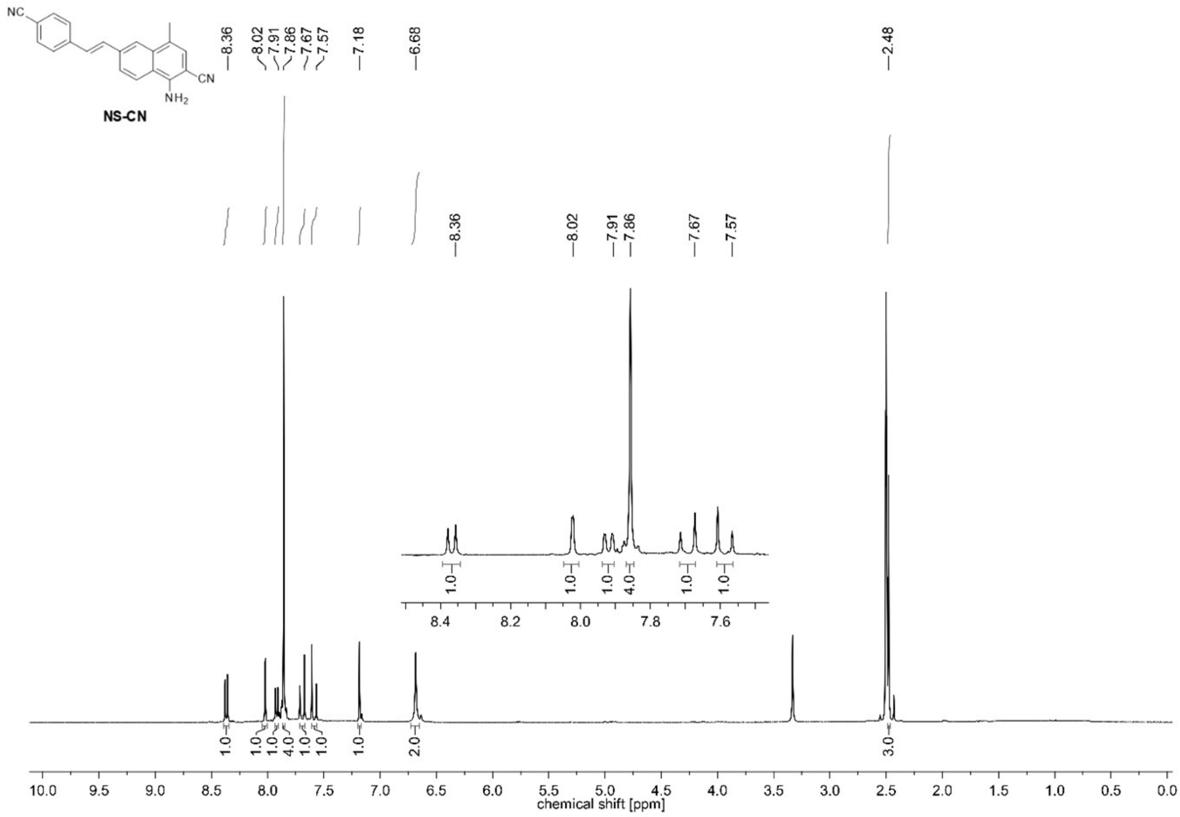

Figure S5. ^{1}HNMR spectrum of 1-amino-6-[(E)-2-(4-cyanophenyl)vinyl]-4-methylnaphthalene-2-carbonitrile, **NS-CN**.

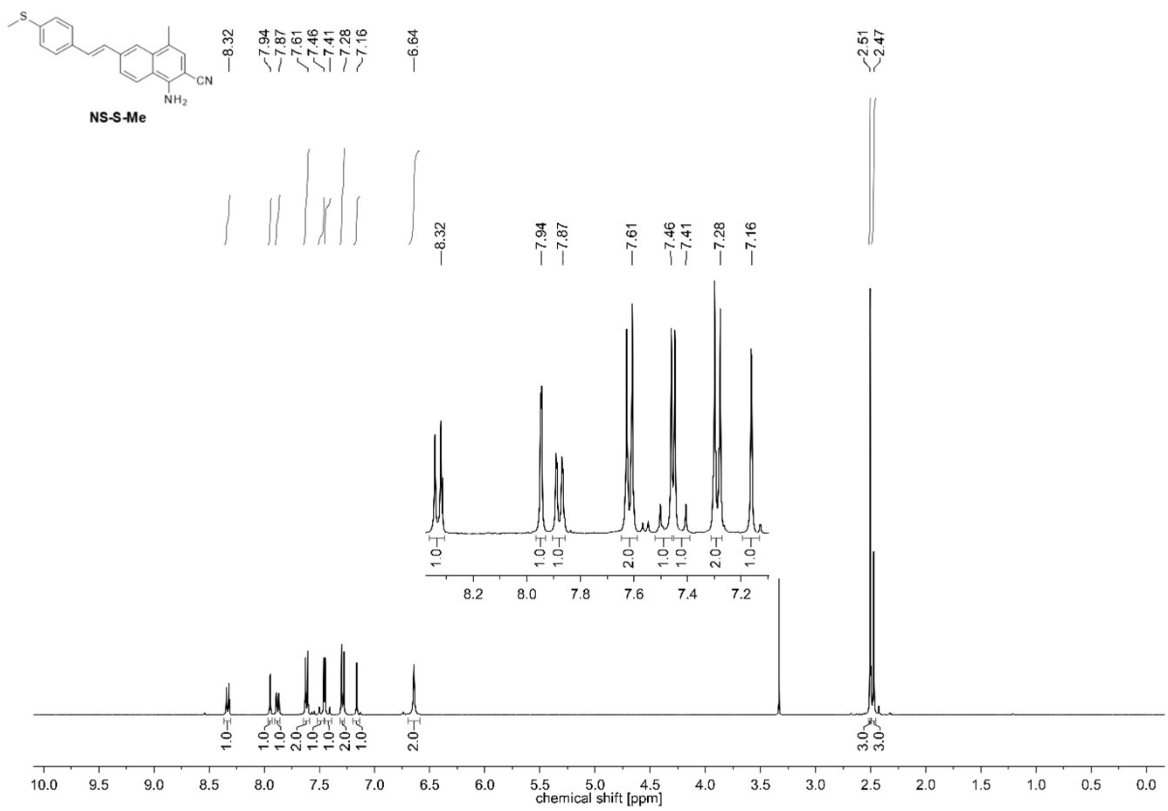

Figure S6. ^{1}HNMR spectrum of 1-amino-4-methyl-6-[(E)-2-(4-methylsulfanylphenyl)vinyl]naphthalene-2-carbonitrile, **NS-S-Me**.

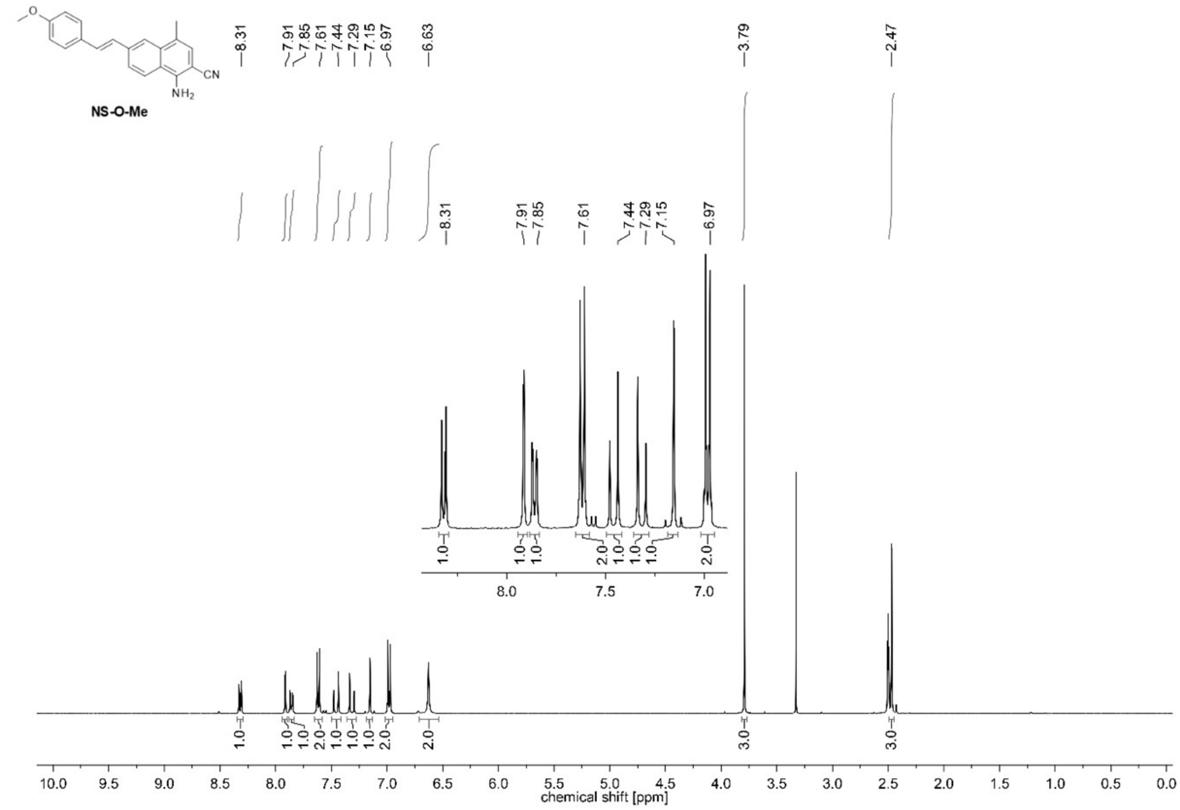

Figure S7. ^{1}HNMR spectrum of 1-amino-6-[(E)-2-(4-methoxyphenyl)vinyl]-4-methylnaphthalene-2-carbonitrile, **NS NS-O-Me**.

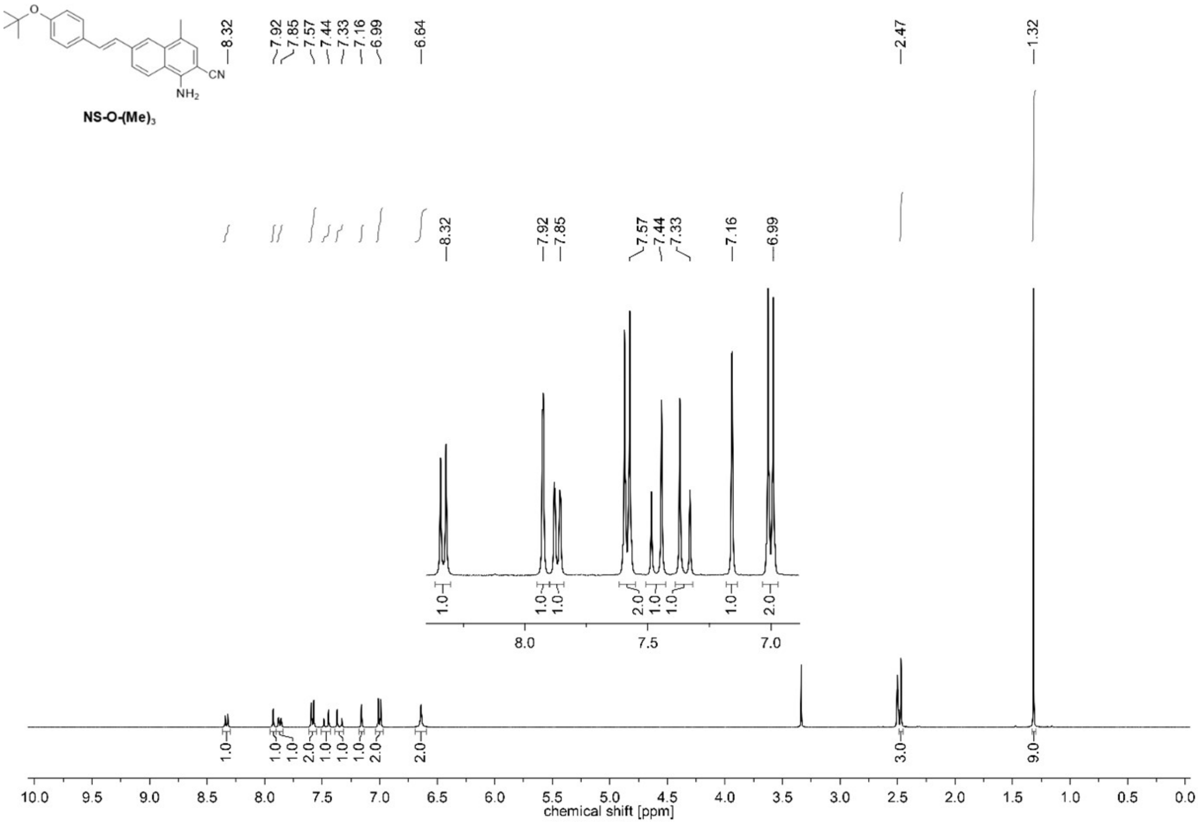

Figure S8. ^{1}HNMR spectrum of 1-amino-6-[(E)-2-(4-tert-butoxyphenyl)vinyl]-4-methylnaphthalene-2-carbonitrile, **NS-O-(Me)$_3$**

Cyclic voltammetry curves showing oxidation and reduction processes of 1-amino-4-methyl-6-styrylnaphthalene-2-carbonitrile derivatives in acetonitrile

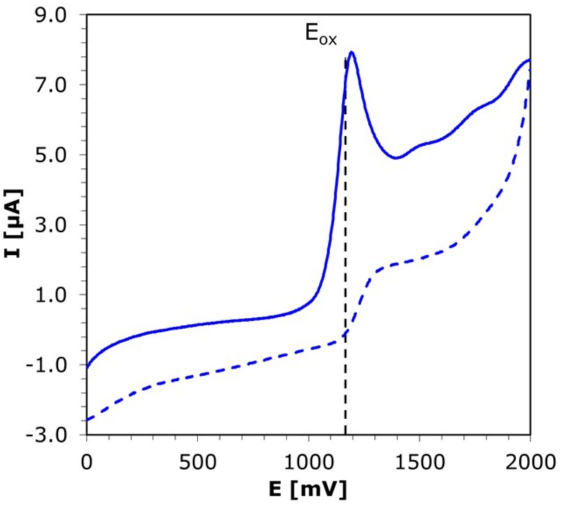

Figure S9: Cyclic voltammogram curves of the NS oxidation in acetonitrile.

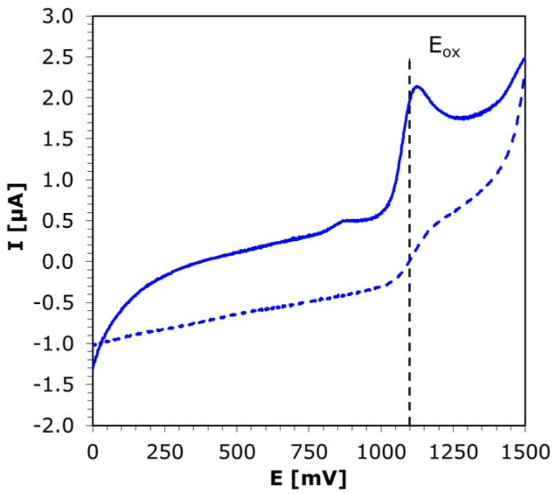

Figure S10: Cyclic voltammogram curves of the NS-Me oxidation in acetonitrile.

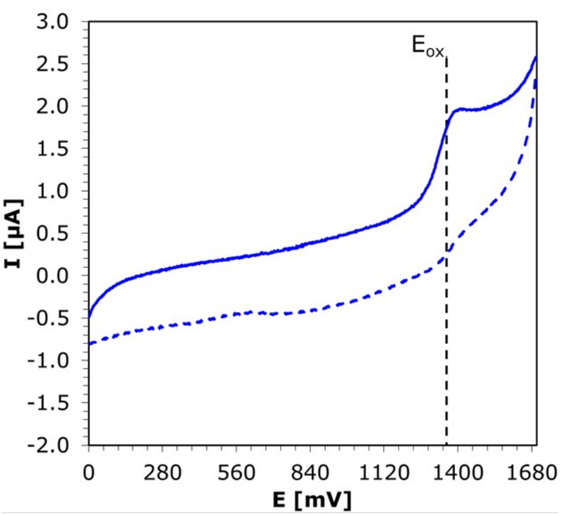

Figure S11: Cyclic voltammogram curves of the NS-F oxidation in acetonitrile.

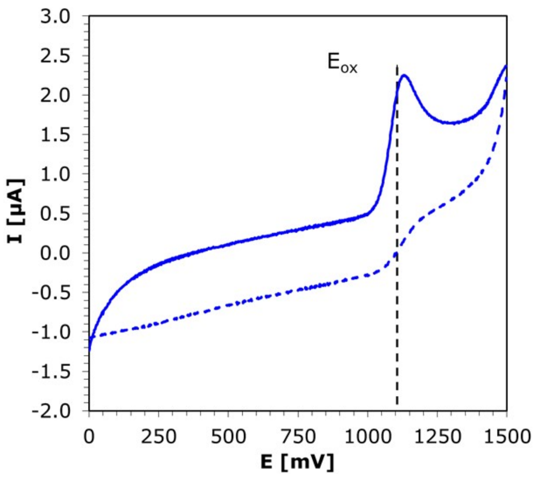

Figure S12: Cyclic voltammogram curves of the NS-Cl oxidation in acetonitrile.

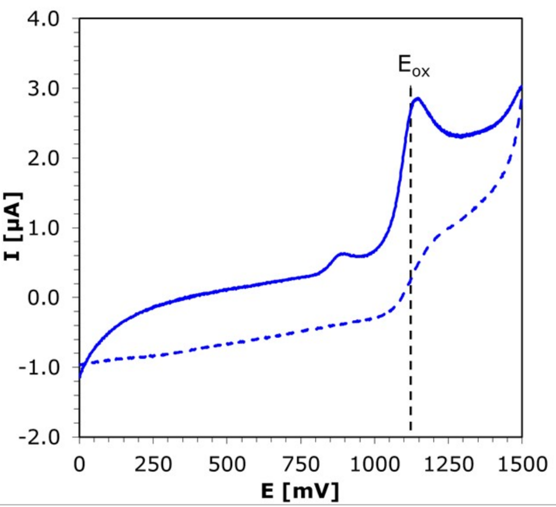

Figure S13: Cyclic voltammogram curves of the NS-CN oxidation in acetonitrile.

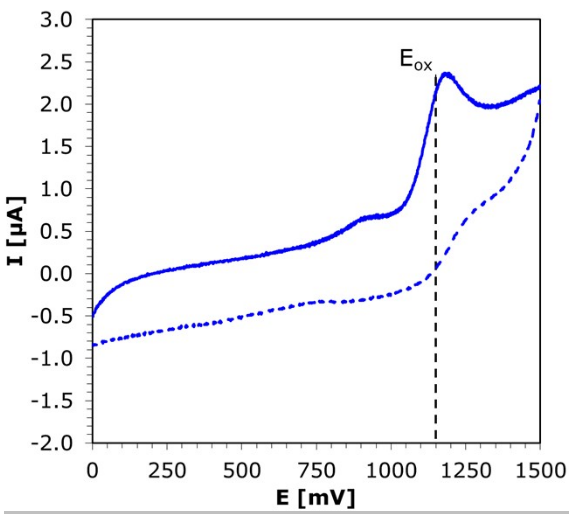

Figure S14: Cyclic voltammogram curves of the NS-S-Me oxidation in acetonitrile.

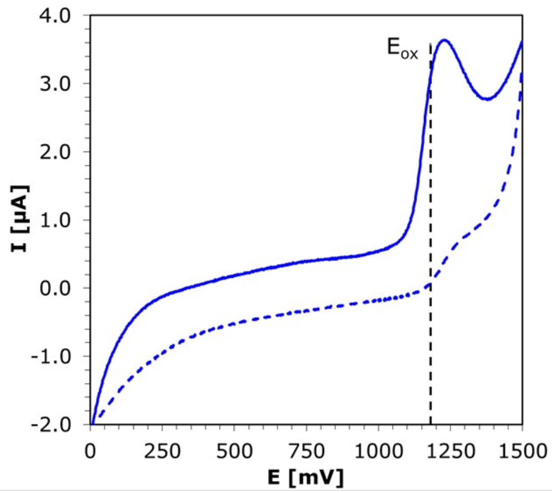

Figure S15: Cyclic voltammogram curves of the NS-O-Me oxidation in acetonitrile.

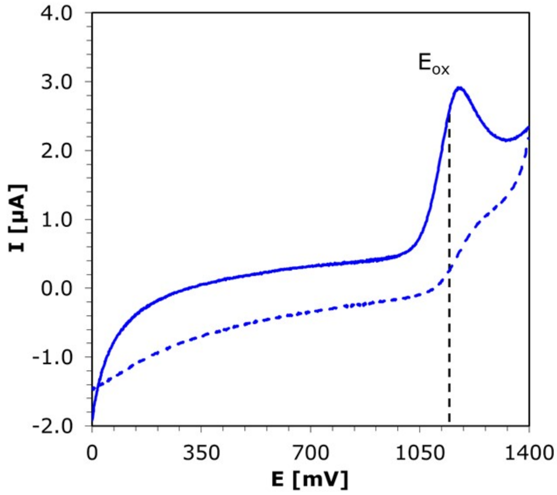

Figure S16: Cyclic voltammogram curves of the NS-O-$(Me)_3$ oxidation in acetonitrile.

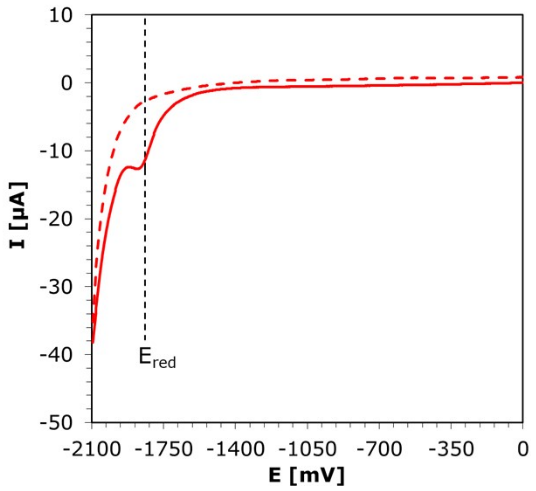

Figure S17: Cyclic voltammogram curves of the NS oxidation in acetonitrile.

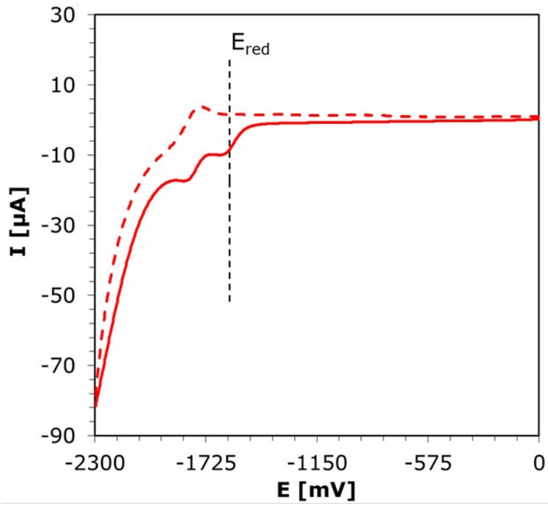

Figure S18: Cyclic voltammogram curves of the NS-CN reduction in acetonitrile.

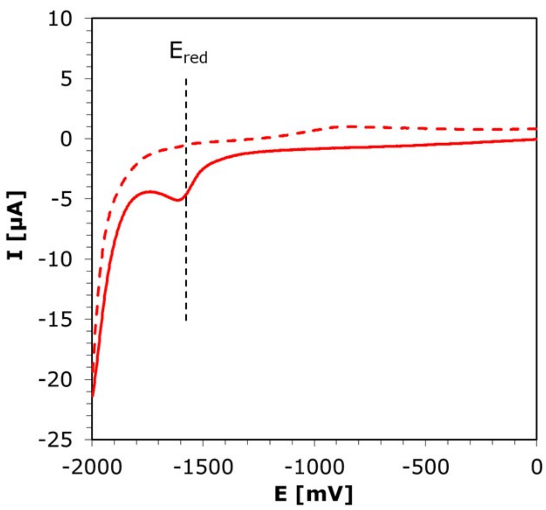

Figure S19: Cyclic voltammogram curves of the NS-O-$(Me)_3$ oxidation in acetonitrile.

Excitation and emission spectra for the determination of the excited singlet state energy for 1-amino-4-methyl-6-styrylnaphthalene-2-carbonitrile derivatives in acetonitrile.

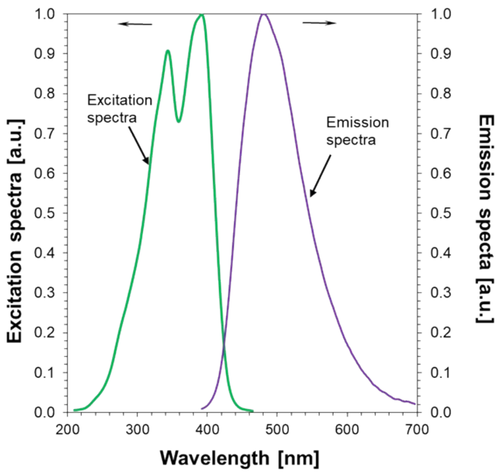

Figure S20: Excitation and emission spectra for the determination of the excited singlet state energy for NS derivative.

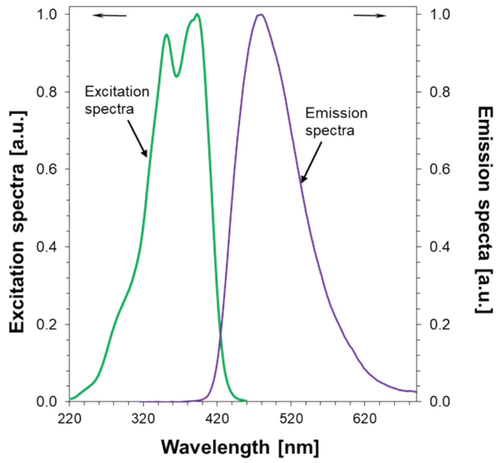

Figure S21: Excitation and emission spectra for the determination of the excited singlet state energy for NS-Me derivative.

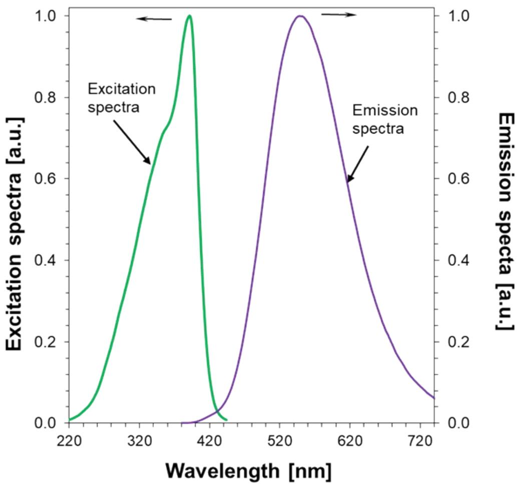

Figure S22: Excitation and emission spectra for the determination of the excited singlet state energy for NS-F derivative.

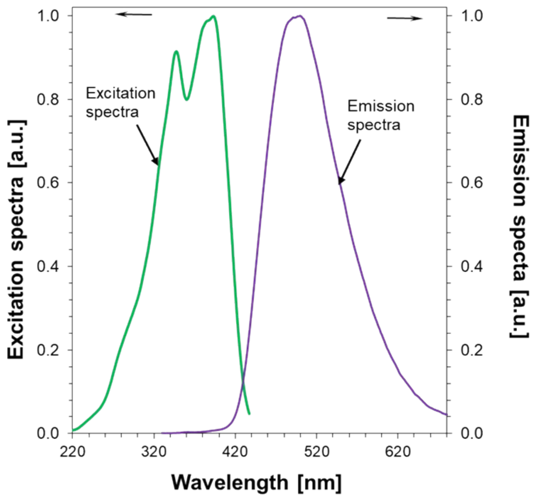

Figure S23: Excitation and emission spectra for the determination of the excited singlet state energy for NS-Cl derivative.

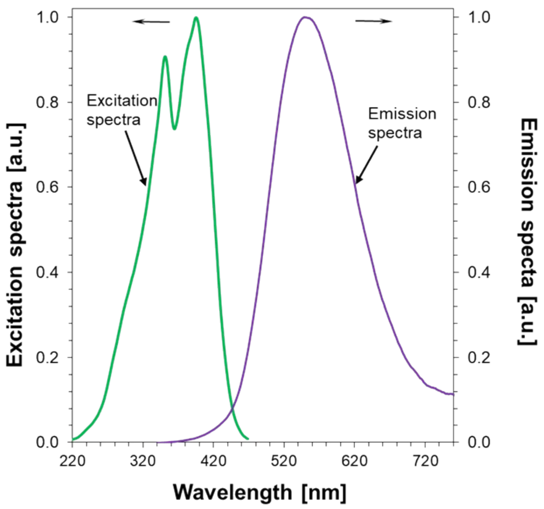

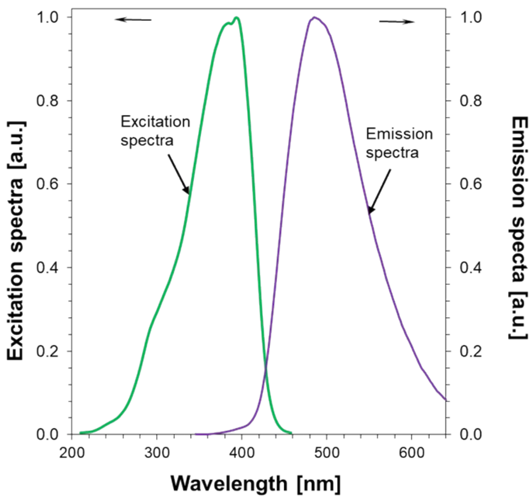

Figure S24: Excitation and emission spectra for the determination of the excited singlet state energy for NS-CN derivative.

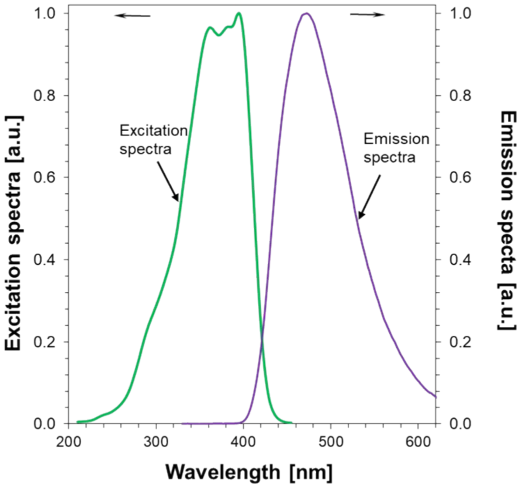

Figure S26: Excitation and emission spectra for the determination of the excited singlet state energy for NS-O-Me derivative.

Figure S25: Excitation and emission spectra for the determination of the excited singlet state energy for NS-S-Me derivative.

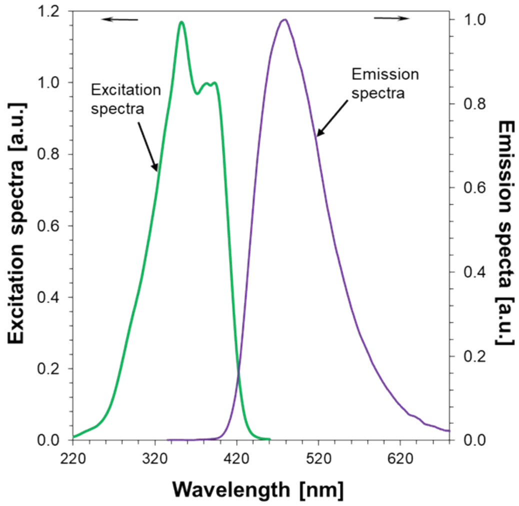

Figure S27: Excitation and emission spectra for the determination of the excited singlet state energy for NS-O-$(Me)_3$ derivative.

Fluorescence quenching of 1-amino-4-methyl-6-styrylnaphthalene-2-carbonitrile derivatives together with Speedcure 938 with Stern-Volmer correlation

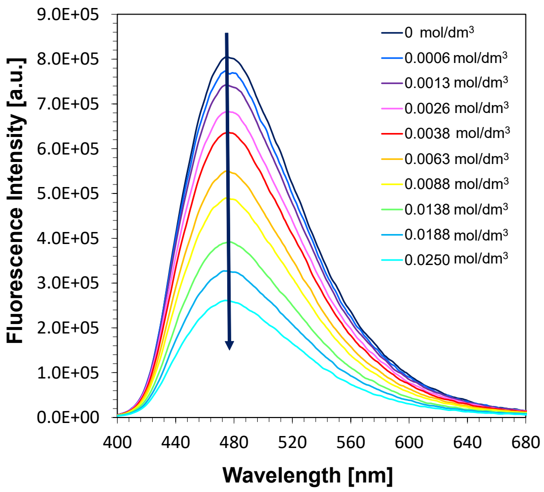

Figure S28: Fluorescence quenching of NS.

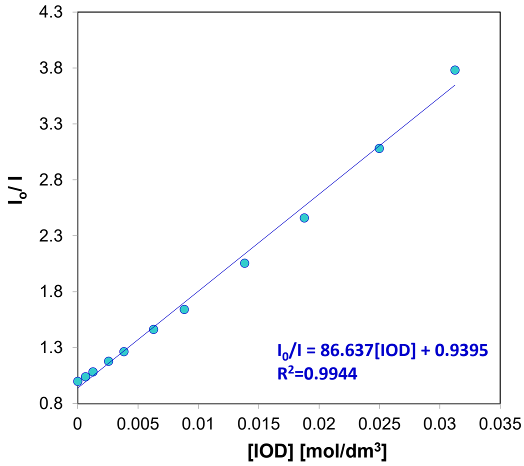

Figure S29: Stern-Volmer treatment for the NS/IOD fluorescence quenching

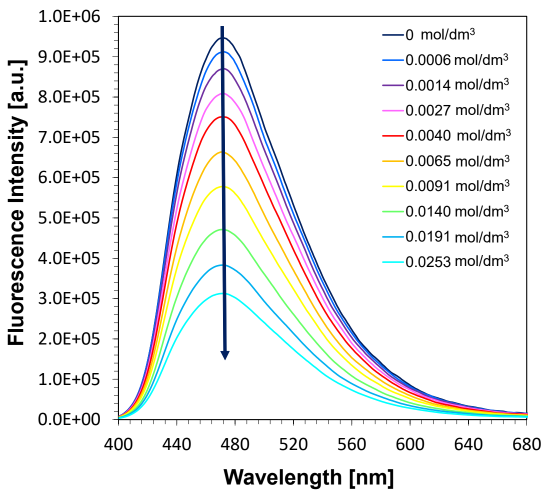

Figure S30: Fluorescence quenching of NS-Me.

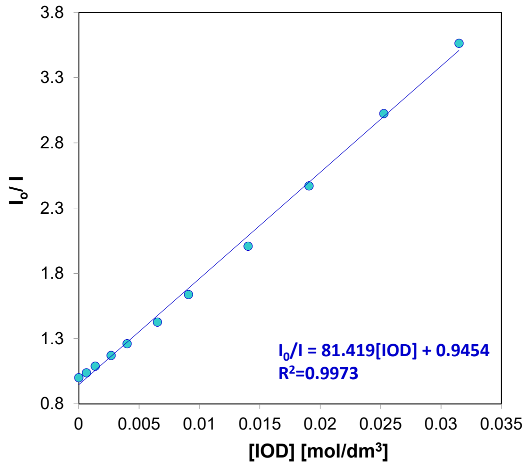

Figure S31: Stern-Volmer treatment for the NS-Me/IOD fluorescence quenching

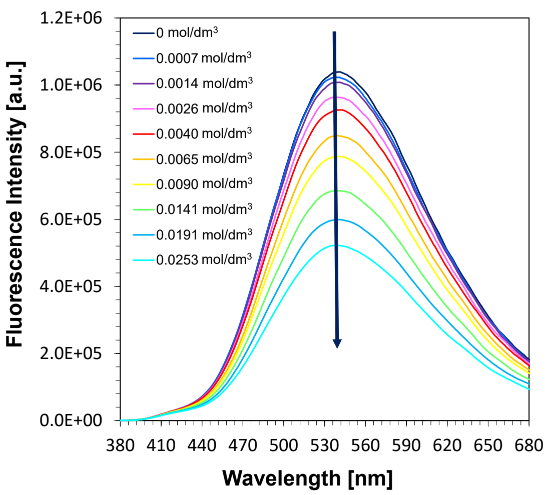

Figure S32: Fluorescence quenching of NS-F.

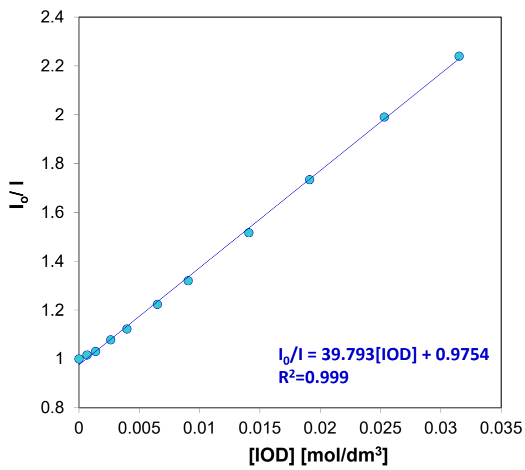

Figure S33: Stern-Volmer treatment for the NS-F/IOD fluorescence quenching

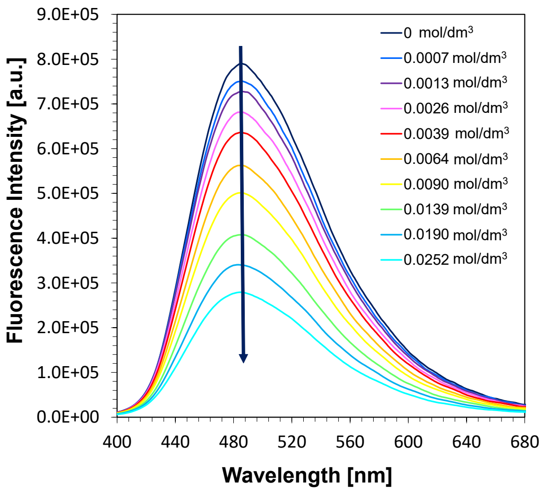

Figure S34: Fluorescence quenching of NS-Cl.

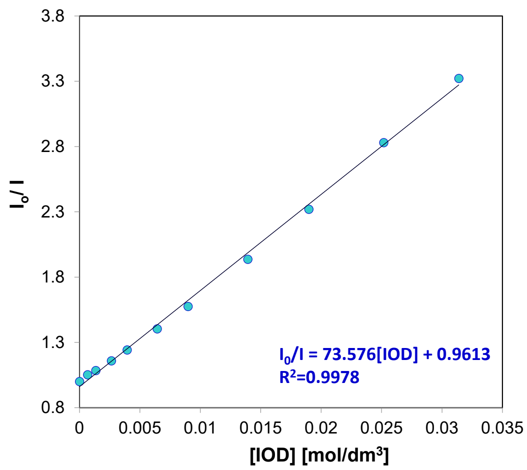

Figure S35: Stern-Volmer treatment for the NS-Cl/IOD fluorescence quenching

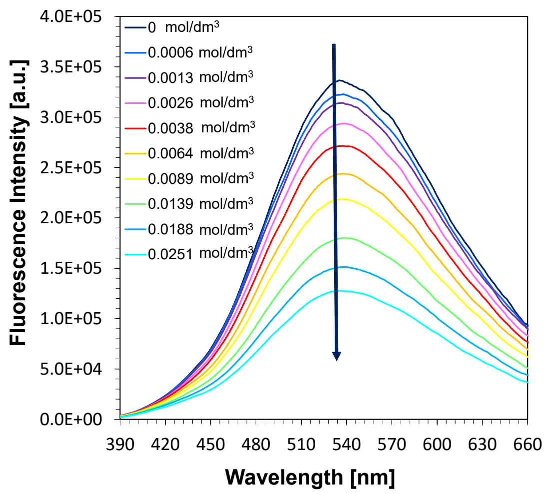

Figure S36: Fluorescence quenching of NS-CN.

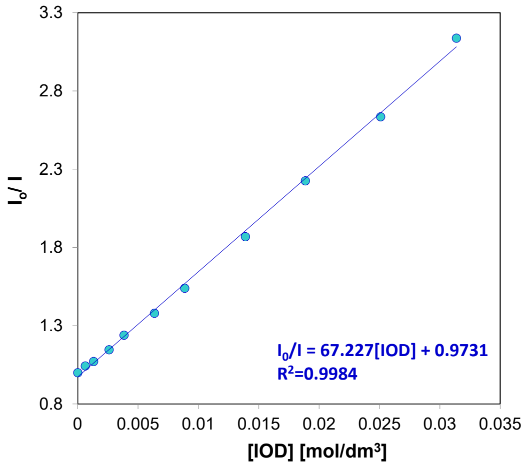

Figure S37: Stern-Volmer treatment for the NS-CN/IOD fluorescence quenching

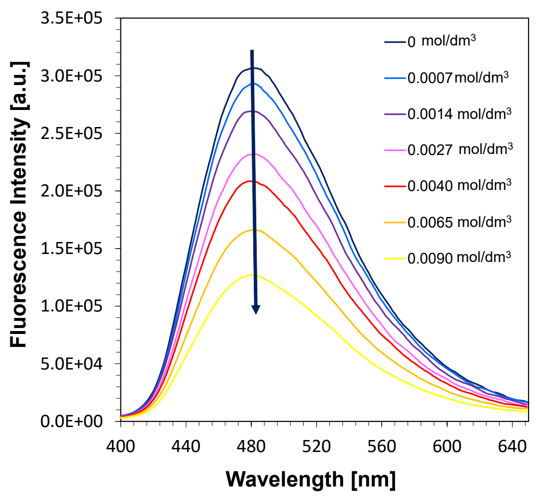

Figure S38: Fluorescence quenching of NS-S-Me.

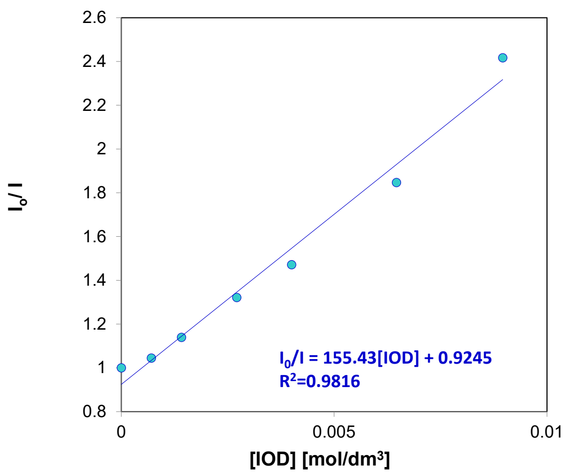

Figure S38: Stern-Volmer treatment for the NS-S-Me/IOD fluorescence quenching

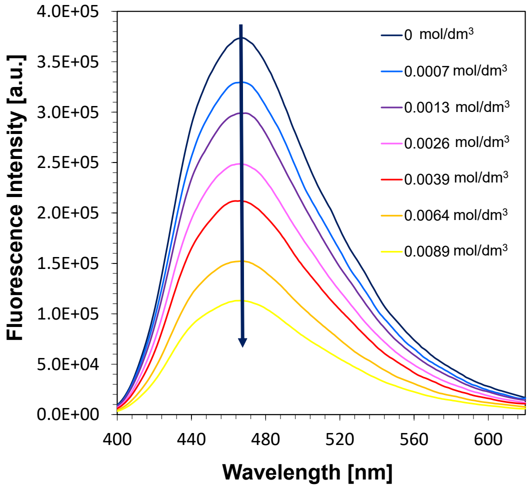

Figure S40: Fluorescence quenching of NS-O-Me.

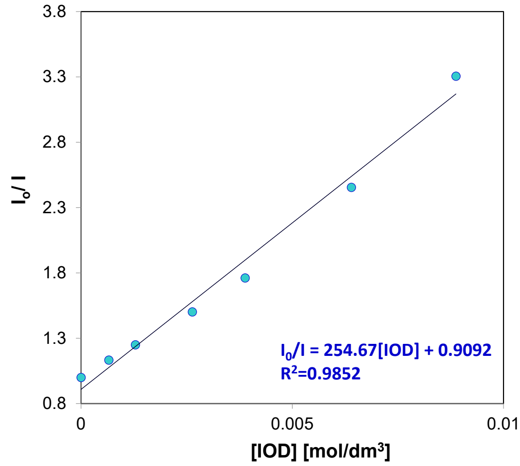

Figure S41: Stern-Volmer treatment for the NS-O-Me/IOD fluorescence quenching

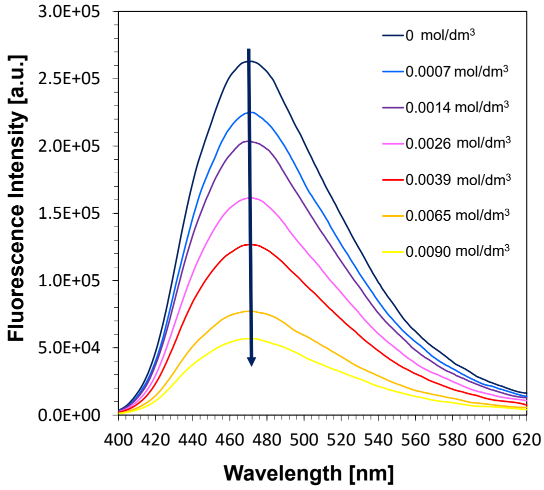

Figure S42: Fluorescence quenching of NS-O-$(Me)_3$.

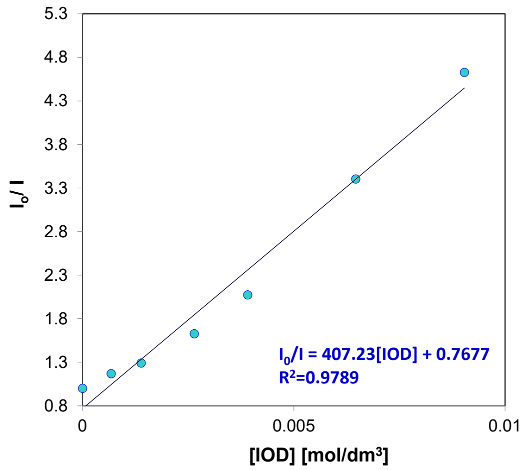

Figure S43: Stern-Volmer treatment for the NS-O-$(Me)_3$/IOD fluorescence quenching

Photolysis of 1-amino-4-methyl-6-styrylnaphthalene-2-carbonitrile derivatives in acetonitrile

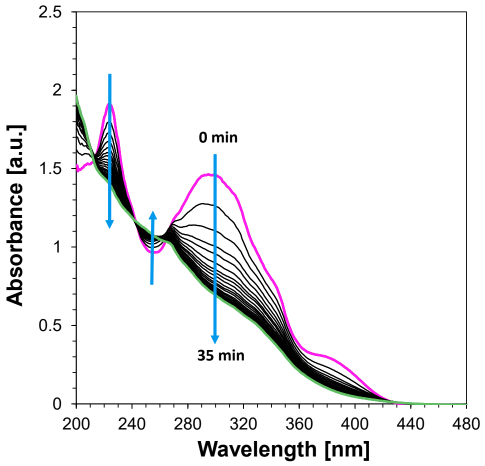

Figure S44: Photolysis of NS in ACN under 405 nm.

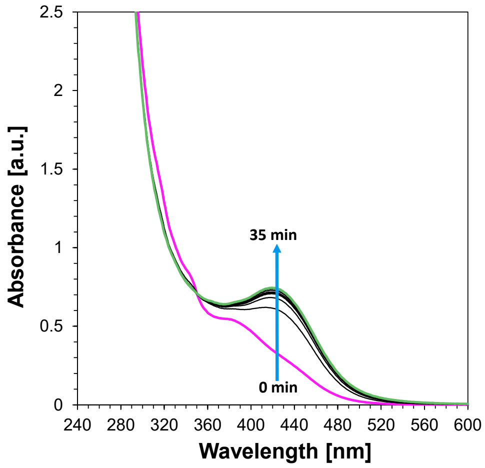

Figure S45: Photolysis of NS + IOD in ACN under 405nm.

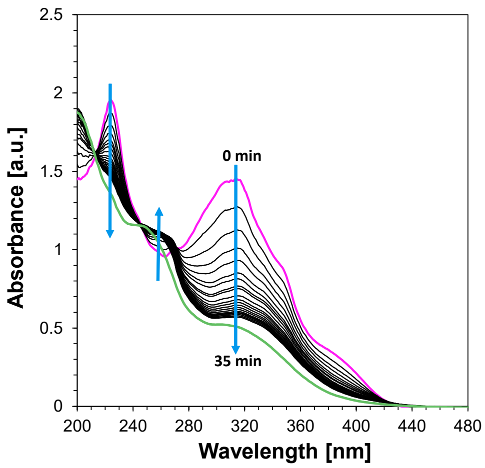

Figure S46: Photolysis of NS-Me in ACN under 405 nm.

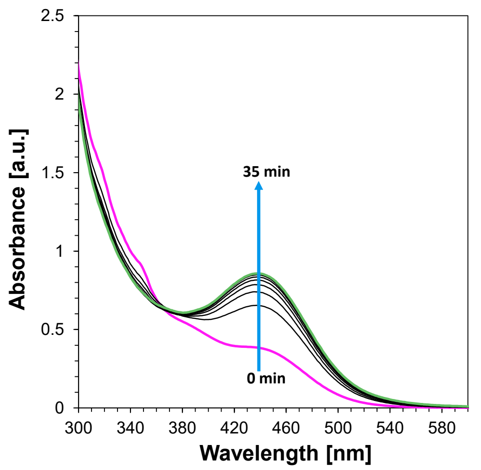

Figure S47: Photolysis of NS-Me + IOD in ACN under 405nm.

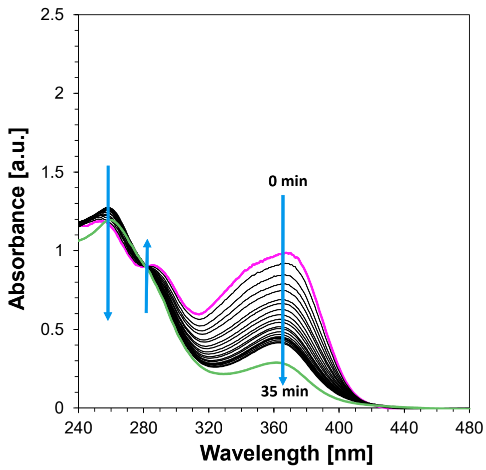

Figure S48: Photolysis of NS-F in ACN under 405 nm.

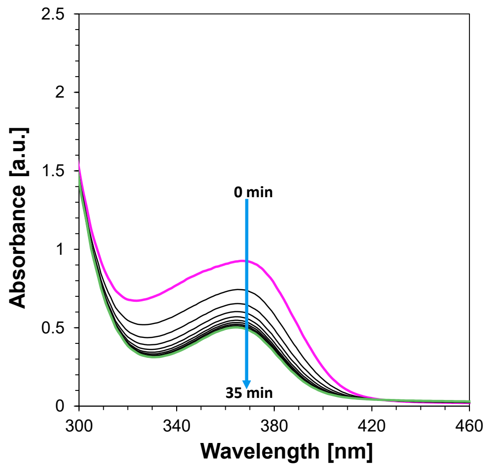

Figure S49: Photolysis of NS-F + IOD in ACN under 405nm.

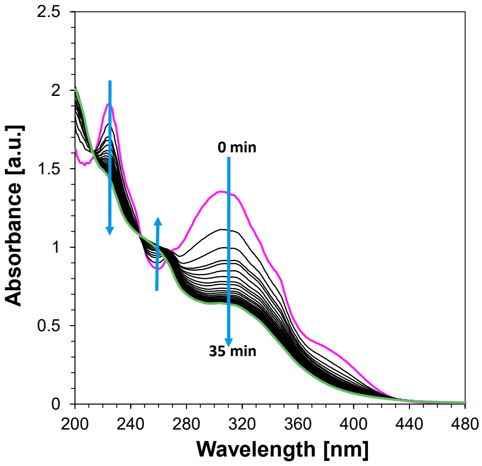

Figure S50: Photolysis of NS-Cl in ACN under 405 nm.

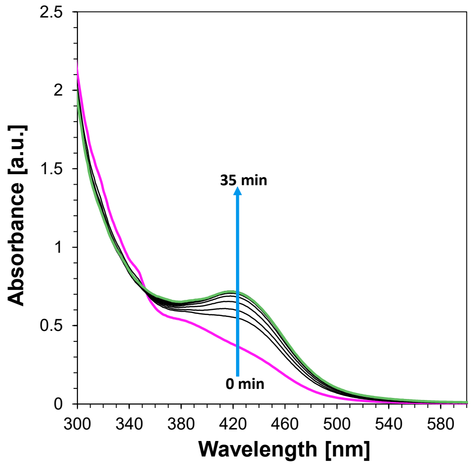

Figure S51: Photolysis of NS-Cl + IOD in ACN under 405nm.

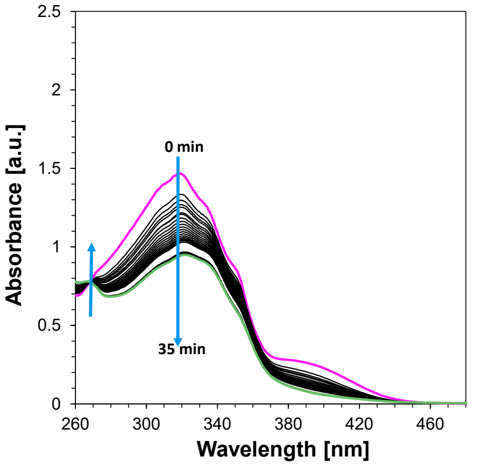

Figure S52: Photolysis of NS-CN in ACN under 405 nm.

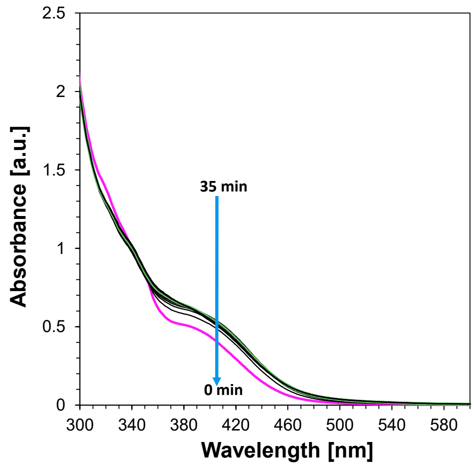

Figure S53: Photolysis of NS-CN + IOD in ACN under 405nm.

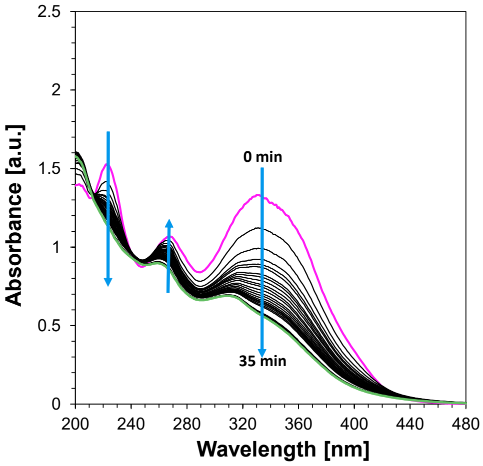

Figure S54: Photolysis of NS-S-Me in ACN under 405 nm.

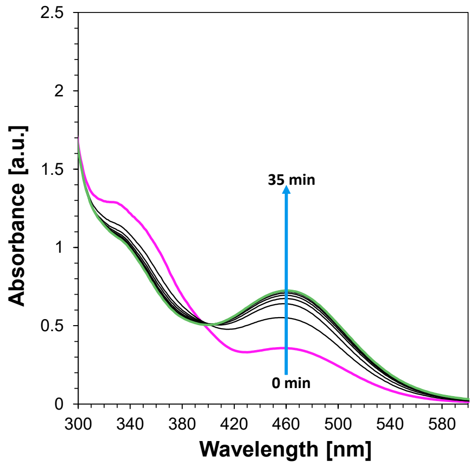

Figure S55: Photolysis of NS-S-Me + IOD in ACN under 405nm.

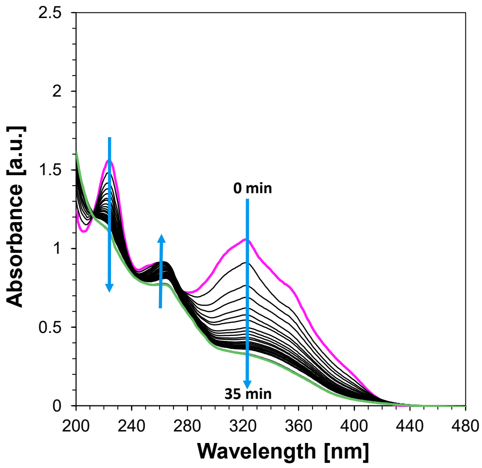

Figure S56: Photolysis of NS-O-Me in ACN under 405 nm.

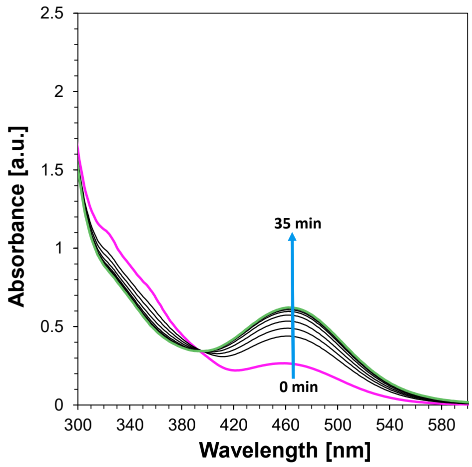

Figure S57: Photolysis of NS-O-Me + IOD in ACN under 405nm.

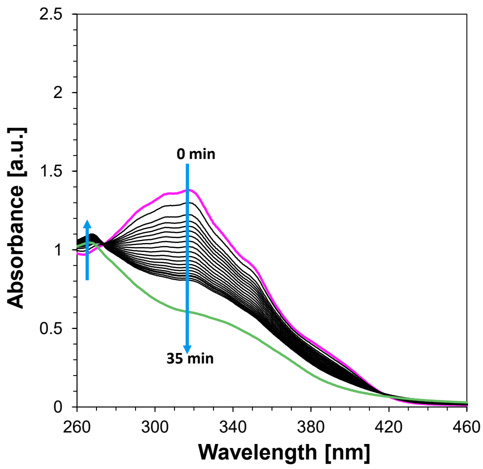

Figure S58: Photolysis of NS-O-$(Me)_3$ in ACN under 405 nm.

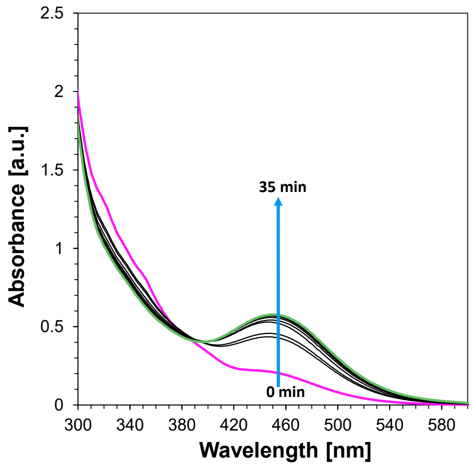

Figure S59: Photolysis of NS-O-$(Me)_3$+ IOD in ACN under 405nm.

FT-IR spectra before and after polymerization for the corresponding reacting bonds/functional groups

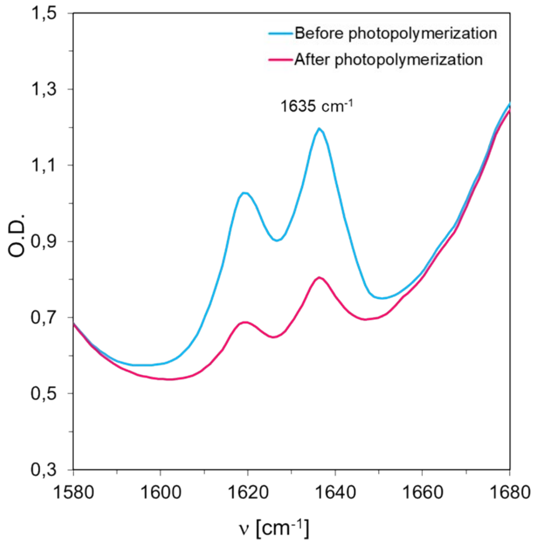

Figure S60: FT-IR spectra before and after polymerization showing the band corresponding to the carbon=carbon bond.

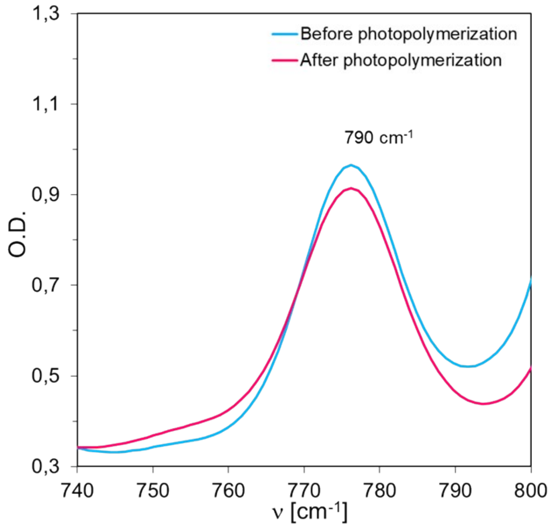

Figure S61: FT-IR spectra before and after polymerization showing the band corresponding to the epoxy group.

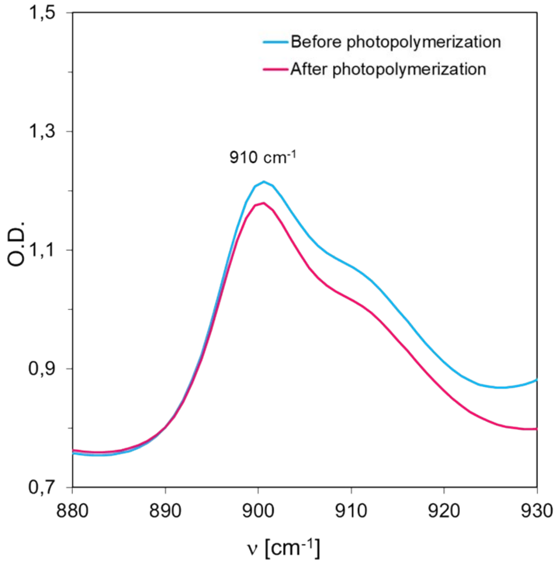

Figure S62: FT-IR spectra before and after polymerization showing the band corresponding to the oxirane group.

Printing parameters

Table S1. Printing parameters for all compositions used on the Anycybic Photon Mono printer.

Sample (acronim)	Thickness of the layer	Curing time of first 4 layers	Curring time of layers
Sample 0	50 [μm]	420 [s]	400 [s]
Sample 1	50 [μm]	200 [s]	150 [s]
Sample 2	50 [μm]	200 [s]	120 [s]
Sample 3	50 [μm]	200 [s]	150 [s]

Table S2. Printing parameters for all compositions used on the LumenX+™ printer.

Sample (acronim)	Thickness of the layer	Curing time of first 4 layers	Curring time of layers	Light power
1% Ag_2O	50 [μm]	15 [s]	5 [s]	90 %
2% Ag_2O	50 [μm]	15 [s]	5 [s]	90 %
5% Ag_2O	50 [μm]	15 [s]	5 [s]	90 %
2% HA	50 [μm]	21 [s]	5 [s]	90 %
5% HA	50 [μm]	21 [s]	5 [s]	90 %
10% HA	50 [μm]	21 [s]	5 [s]	90 %

Printing of specimens for DMA

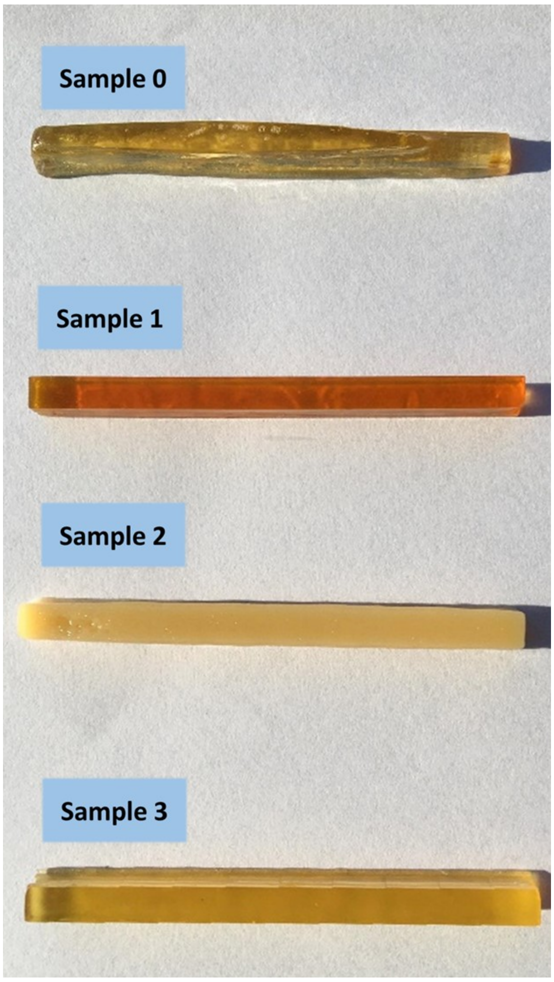

Figure S63: Photos of specimens printed for DMA testing.

SEM

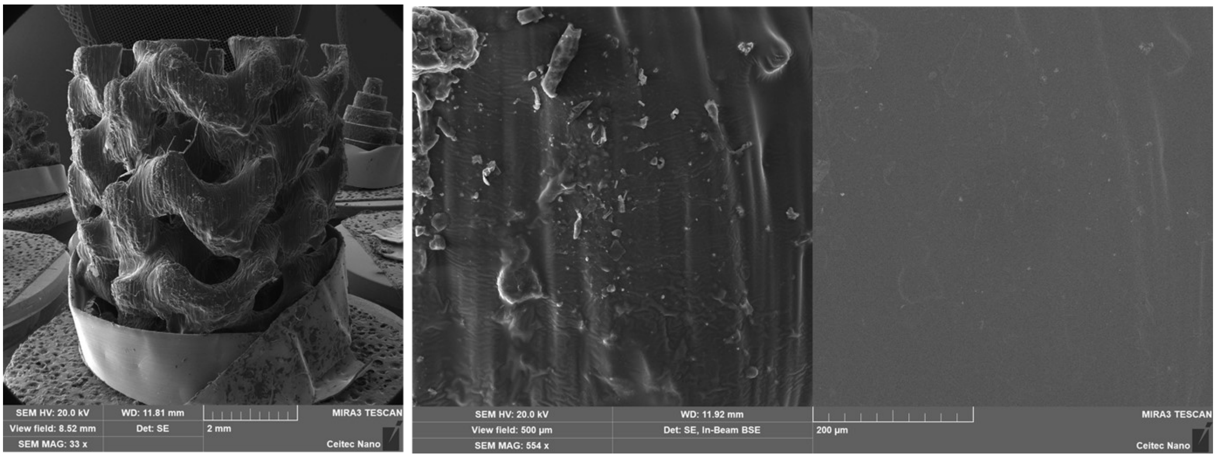

Figure S64: SEM analysis of nanocomposite: Ebecryl® 4858/IBOA (0.7/0.3 w/w) + IOD/NS (3.0/0.1 w/w) + 1% of Ag_2O.

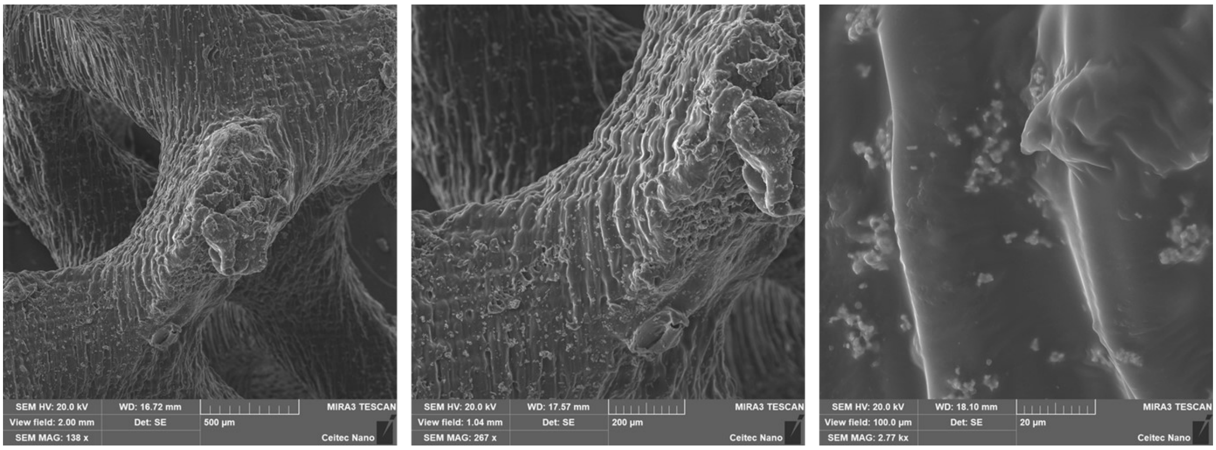

Figure S65: SEM analysis of nanocomposite: Ebecryl® 4858/IBOA (0.7/0.3 w/w) + IOD/NS (3.0/0.1 w/w) + 5% of Ag_2O.

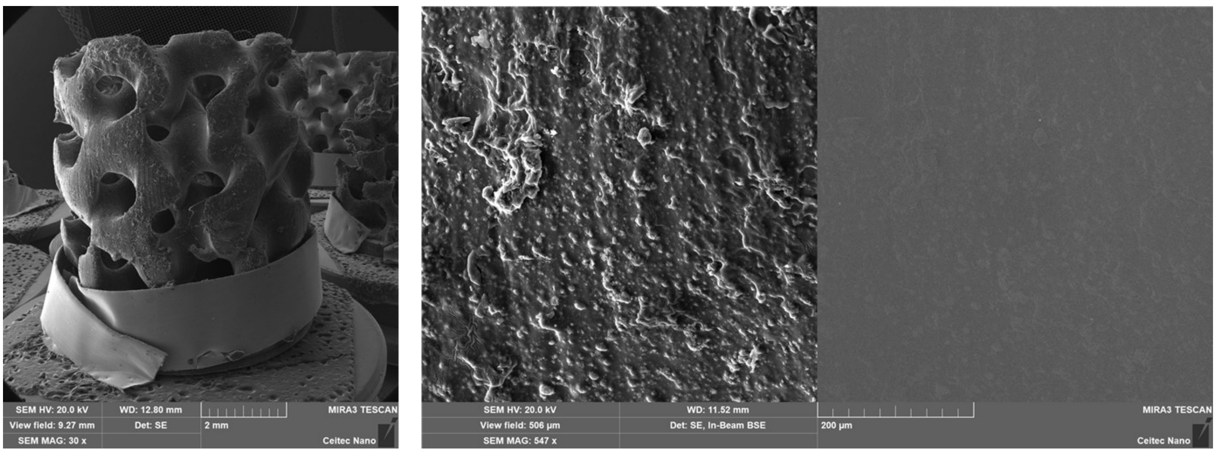

Figure S66: SEM analysis of nanocomposite: Ebecryl® 4858/IBOA (0.7/0.3 w/w) + IOD/NS (3.0/0.1 w/w) + 2% of HA.

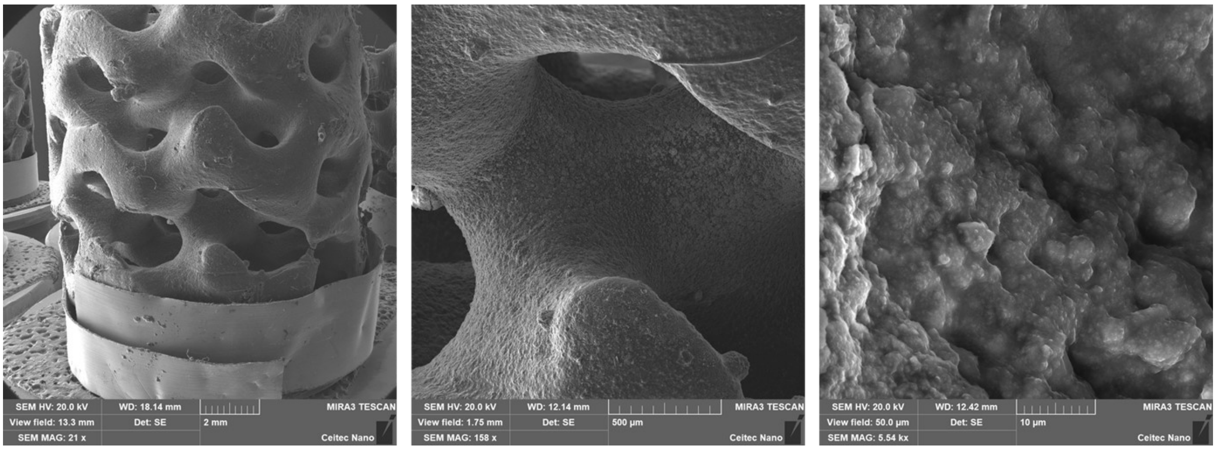

Figure S67: SEM analysis of nanocomposite: Ebecryl® 4858/IBOA (0.7/0.3 w/w) + IOD/NS (3.0/0.1 w/w) + 5% of HA.

Literature

[1] E. Hola, M. Topa, A. Chachaj-Brekiesz, M. Pilch, P. Fiedor, M. Galek, J. Ortyl, New, highly versatile bimolecular photoinitiating systems for free-radical, cationic and thiol–ene photopolymerization processes under low light intensity UV and visible LEDs for 3D printing application, RSC Adv. 10 (2020) 7509–7522. https://doi.org/10.1039/C9RA10212D.

[2] W. Tomal, M. Pilch, A. Chachaj-Brekiesz, M. Galek, F. Morlet-Savary, B. Graff, C. Dietlin, J. Lalevée, J. Ortyl, Photoinitiator-catalyst systems based on meta-terphenyl derivatives as photosensitisers of iodonium and thianthrenium salts for visible photopolymerization in 3D printing processes, Polym Chem. 11 (2020) 4604–4621. https://doi.org/10.1039/D0PY00597E.